EIGHTH HEART OF EUROPE BIO-CRYSTALLOGRAPHY MEETING

Karlovy Vary, September 29 - October 1, 2005

Lectures - Thursday, September 29

L1

FOUR CRYSTAL FORMS OF A BACTERIAL DEHYDROGENASE WITH A DISORDER OR TWINNING PROBLEM?

Karthik S. Paithankar and Norbert Sträter

Biotechnologisch-Biomedizinisches Zentrum, Fakultät für Chemie und Mineralogie, Universität Leipzig, Deutscher Platz 5, D-04103, Germany. karthik@bbz.uni-leipzig.de

The short-chain dehydrogenases (SDR) belong to the large family of NAD- or NADP-dependent oxidoreductases consisting of about 250 residues. They typically exhibit sequence identities at 15 – 30% level, indicating extensive divergence. R-3-hydroxybutyrate dehydrogenase (HBDH) from *Pseudomonas putida* reversibly oxidizes 3-hydroxybutyrate to acetoacetate using NAD as coenzyme. Crystallization of HBDH by hanging-drop method using PEG1500 yields rectangular crystals of dimensions 0.1 0.2 0.2 mm. Under similar conditions we have obtained four different crystal forms, which diffract up to 1.9 Å resolution. All four crystal forms can be indexed in a C centered monoclinic lattice, crystal form IV however belongs to Laue class -1. Molecular replacement with a homologous structure of 30% identity (*AMoRe*) yields a solution for all crystal forms, with a content of between 2 and 8 monomers of the 222 tetramer in the asymmetric unit. All four crystal forms have unusually low solvent contents between close to 0 and 23.5 %. The molecular replacement solutions and density maps show no obvious overlap of the models. Despite the high non-crystallographic symmetry, the density maps hardly improve by phase refinement. Also the R_{free}-factor remains about 40%, even after parts of the model have been rebuild on the basis of the density which is reasonably defined in the core of the protein but bad in some contact regions. Although, the intensity statistics do not indicate twinning, the above facts indicate that there is a related disorder or twinning problem with all of these crystals.

1. Joernvall, H., *et al.,* Short-chain dehydrogenases/reductases (SDR) (1995). *Biochemistry* **34**, 6003-6013.
2. Persson, N., *et al.,* Characteristics of short-chain alcohol dehydrogenases and related enzymes (1991). *Eur J. Biochem* **200**, 537-543.

L2

-HELIX ORIENTATION DIRECTLY FROM THE DIFFRACTION PATTERN

Grzegorz Chojnowski[1,2,3] and Matthias Bochtler[1,2]

[1]*International Institute of Molecular and Cell Biology, ul. Trojdena 4, 02-109 Warsaw, Poland*

[2]*Max-Planck-Institute for Molecular Cell Biology and Genetics, Pfotenhauerstr. 108, 01309 Dresden, Germany*

[3]*Department of Biophysics, Warsaw University, Zwirki i Wigury 93, 02-089 Warsaw, Poland*

-helices are key building blocks of peptides and proteins. In X-ray diffraction experiments, they give rise to very prominent reflections in the directions parallel and antiparallel to the helix axis at 1.5 Å resolution, because the contributions from all helix residues add in phase. In the early days of protein crystallography, the location of the 1.5 Å reflection was crucial to deduce and confirm Pauling's model for the -helix, but today no special attention is paid to this prominent reflection. Here, we derive estimates for the intensities and shapes of the 1.5 Å reflections from individual a-helices in proteins, and show that these reflections are sufficiently strong to be sometimes recognizable in the 3D-diffraction patterns of crystals that diffract to better than 1.5 Å resolution. We have implemented and benchmarked the program OPF (OnePointFive) that searches for such reflections in the 3D-diffraction patterns of protein crystals. In favorable cases, the program can deduce helix orientations, which could not be deduced by molecular replacement with idealized model helices.

L3

AUTO-RICKSHAW: AUTOMATED CRYSTAL STRUCTURE DETERMINATION AS AN EFFICIENT TOOL TO VALIDATE AN X-RAY DIFFRACTION EXPERIMENT

S. Panjikar, V. Parthasarathy, V. S. Lamzin, M. S. Weiss and P. A. Tucker

European Molecular Biology Laboratory, Notkestrasse 85, D-22603 Hamburg, Germany

Auto-Rickshaw [1] is a system for automated crystal structure determination. It provides computer coded decision-makers for successive and automated execution of a number of existing macromolecular crystallographic computer programs thus forming a software pipeline for automated and efficient crystal structure determination. *Auto-Rickshaw* can be started as soon as X-ray data from derivatised protein crystals have been collected and processed.

Auto-Rickshaw is invoked through a web-based graphical user interface (GUI) for data and parameter input, and for monitoring the progress of structure determination. A large number of possible structure solution paths are encoded in the system and the optimal path is selected by the decision-makers as the structure solution evolves. The processes have been optimised for speed, so that the pipeline can be used effectively for validating the X-ray experiment at a synchrotron beamline. Currently, the platform is restricted to SAD, SIRAS, 2W-MAD, 3W-MAD or 4W-MAD phase determination.

Important parameters are entered (e.g. name of project, space group, number of residues per monomer, number of heavy atoms per monomer, number of monomer(s) in the asymmetric unit) and the desired phasing protocol is chosen. Each procedure combines data preparation, substructure solution, heavy atom refinement, phase calculation, density modification, non-crystallographic symmetry (NCS) averaging and partial model building. Once important parameters are entered, X-ray derivative data are loaded and the process is invoked by pressing the "submit" button. No further user intervention is needed.

The platform is installed on a 16-processor Linux cluster and the server [2] is accessible from most Internet browsers and allows Hamburg beamline users and EMBL staffs to validate their X-ray diffraction experiments in the shortest possible time.

1. Panjikar, S., Parthasarathy, V., Lamzin, V. S., Weiss, M. S. & Tucker, P. A. (2005). *Auto-Rickshaw* - An automated crystal structure determination platform as an efficient tool for the validation of an X-ray diffraction experiment. *Acta Cryst.* **D61**, 449-457.

2. http://www.embl-hamburg.de/Auto-Rickshaw/.

L5

UTILIZATION OF FREE-RADICAL SCAVENGERS FOR THE REDUCTION OF RADIATION DAMAGE DURING DATA COLLECTION

B. Kauffmann, M.S. Weiss, V. S. Lamzin and A. Schmidt

European Molecular Biology Laboratory, Notkestrasse 85, D-22603 Hamburg, Germany

Radiation damage is thought to be the underlying cause of most unsuccessful MAD experiments [1]. In addition to general damage effects such as increased mosaicity, R_{merge}, Wilson *B* factors, and loss of resolution, specific structural radiation damage has also been shown to occur in proteins. This includes the breaking of disulfide bonds and the loss of carboxylate groups from aspartate and glutamate residues [2]. Radiation damage can be described as primary (photon interacts inelastically with an atomic electron within the crystal, energy is absorbed) or secondary (creation of radicals species and secondary electrons which then react to produce further damage). Although it may be difficult to limit the primary radiation damage, parameters that may affect the rate of secondary damage are more amenable to modification by experimenters. Macromolecular crystals are routinely cooled to 100K to reduce the mobility of radiation-induced free radicals. Some radical species, in particular electrons, are still mobile at 100 K [3]. Radical scavengers may be able to interact with these species, reducing both their mobility and their reactivity, and may also be able to facilitate the neutralization of immobile ionized groups formed in primary and secondary events. Many potential scavengers for protein crystals have been mentioned in the literature, although very few have been tested experimentally [1].

We will present our investigations on the use by quick soaking of three different molecules (nicotinic acid, oxidized glutathion and DTNB) on three different crystal models (lysozyme, elastase and thaumatin) to reduce the radiation damage (Figure 1). We will present also our results on the impact of radiation damage on glycerol, commonly used as cryoprotectant.

1. J. Murray and E. Garman, (2002). *J Synchr. Rad.* **9**, 347-354.

2. M. Weik, R. B. Ravelli, G. Kryger, S. McSweeney, M. L. Raves, M. Harel, P. Gros, I. Silman, J. Kroon and J. L. Sussman (2000). *Proc. Natl. Acad. Sci. USA* **97**, 623-628.

3. G. D. D. Jones, J. S. Lea, M. C. R. Symons and F. A. Taiwo (1987). *Nature* **330**, 772-773.

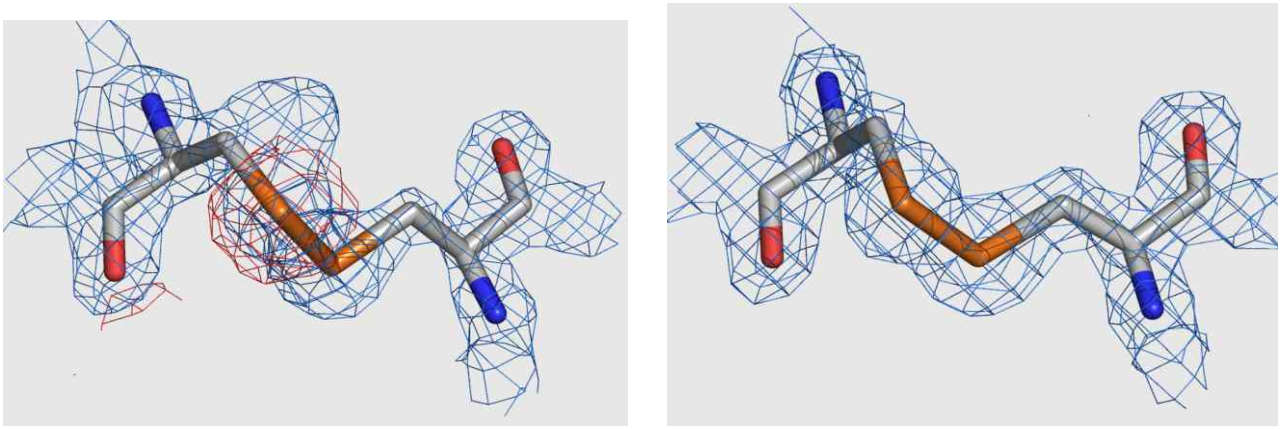

Figure 1. Disulfide bridge broken in the native lysozyme crystal after 5 times 360 (left). On the right, the same disulfide bridge after 5 times 360 for the crystal soaked in a 200 mM nicotinic acid. The maps shown are the 2fofc-map (blue) and the fofc-map (red contoured at 1.5 and 3 respectively.

L6

HIPHOP. A NOVEL REFINEMENT METHOD FOR PROTEIN STRUCTURES

J. Ondráček

Department of Recombinant Expression and Structural Biology, Institute of Molecular Genetics, Academy of Sciences of the Czech Republic, Flemingovo n. 2, CZ-16637 Praha 6, Czech Republic

During the refinement process last structure details are modeled and structure parameters minimized. The refinement process is usually stopped in the minimum on the refinement curve. Every possible model has its own refinement curve and every refinement curve is in fact a function of the Fourier transform of the X-ray diffraction data. Only one electron density corresponds to our request on the quality of the final model.

For proteins, usually only limited resolution data are available and the Fourier transform of such data is poor due to low number of Fourier coefficients in comparison to those of full resolution small molecule structures. Minima on the optimal protein refinement curve are not so frequent and deep. This is why reliability factors for proteins must be higher then those for small molecules. Furthermore, it is impossible to distinguish the global minimum between many local ones.

During the refinement process the refinement curves can lie above or bellow the optimal refinement curve. The refinement curve will lie above in the first steps of the model buildings and refinements or when the resolutions are increased during the refinements. In these cases the models are under-parameterized. During refinements, values of reliability factors must decrease. Reverse situation is when higher resolution model is used as the initial model or when the resolution during the refinement is decreased. In these cases models are over-parameterized (over-determined or over-refined) and during the rebuilding and refinement the number of refined parameters must be reduced and thus, reliability factors must increase.

The power of the refinement method used depends on its possibility to reach the optimal refinement curve and to determine the deepest minimum on it. Usually, the refinement process is not able to overcome higher barriers on the refinement curve if no significant attempts of the model improvement are made (the model is only little over-parameterized) and the new refined model is very similar to the old one. Then, the local minimum reached is very close to previous one. When huge structural change on the model is made the refinement process is able to overcome huge barriers on the refinement curve and the radius, in which the refinement method used is able to reach the best minimum, increases.

The HipHop refinement is based on the repeating of the huge structural changes and refinements followed by several structure reducing and refinement cycles. This is repeated until the values of reliability factors and water content are stable within statistical variances. The result of the HipHop refinement is not one single model of electron density (as usual) but a set of possible solutions in local minima corresponding to a set of possible electron densities.

One HipHop step usually consists of one Hip and several Hop steps. Every Hip/Hop step is followed by the refinement.

The Hip (excitation) step is carried out by adding of proper number of waters corresponding to the maxima in the difference Fourier map. Suitable number of waters is usually ~ 15 % of non-hydrogen protein atoms with the occupancy 0.5 and thermal parameter U = 1.2 for Shelxh or B = 30 for Refmac5 version. So the higher the number of waters added do the model is and the lower their thermal parameters are the higher the radius for the location of a minimum is. On the other hand this is limited by the refinement stability. By the use of the parameter described the phase change is usually ~ 1 %. The model is in this way

over-parameterized due to new possible water positions and during the refinement cycles the new model with new main/side chain orientation and new set of water molecules is formed. Shifts of water positions in first refinement steps are about 2-3 Å.

In the Hop (reduction) step wrong waters are removed from the model. The Hop step is repeated usually five times and in every step the minimal electron density limit is increased five times. Water is considered to be wrong when 1) the calculated electron density in the water position is lower then the limit given for the step, 2) the water does not have the ball shape and 3) the water is too close to the protein molecule.

One run of HipHop usually consists of ten HipHop steps. After this, the stability of reliability parameters, number of water molecules in the model, and the agreement of the electron density with the model are evaluated. If necessary, the model improvement is done manually and the HipHop run is repeated until the reliability parameters and number of waters is stable and no possible structure improvement appears.

The final stability of the HipHop refinement is the proof of the correctness of the method used for the refinement. The HipHop refinement yields classical R and R_{free} factors. Except those, it is useful to define and calculate the Refinement Reliability Factor R_{rrf}. This is defined in the same way as R_{free} with the exception that the reflections used for R_{rrf} calculation can be used in previous refinement steps. Final average value of R_{rrf} is usually similar to R_{free} . The exclusivity of reflections used for the R_{free} calculation is substituted by the statistical evaluation of R_{rrf}s by the calculation of its final value by the use of phase average after HipHop refinement.

During the tests of HipHop refinement method on several protein X-ray data no one unique solution which would have statistically better reliability factors than the rest of possible solutions was found. Structural variances yielded by HipHop refinement correspond to the resolution and the quality of the X-ray data.

L7

CURRENT STATUS AND DEVELOPMENT PLANS OF THE BESSY PX BEAMLINES

Uwe Mueller, Martin Fieber-Erdmann, Martin Fuchs & Ronald Förster

BESSY GmbH, Albert-Einstein-Str. 15, 12489-Berlin, Germany

Since 2002, the Berlin third generation electron storage ring BESSY and the Free University Berlin operate two tuneable energy macromolecular X-ray diffraction beamlines [1]. So far, the successful operation of this installation led to 53 PDB entries from experimental beam time of over 50 international user groups. The Berlin area based structural biology user community is intensively using the BESSY beamlines, i.e. the annual amount of granted beam time corresponds to a total of 150 8h-shifts.

Within this year, the new BESSY digital user office BOAT (www.bessy.de/boat/www) will enhance its functionality and is a modern tool for the planning, application and operation of experimental beam time at BESSY.

For the next 24 months we plan to perform a major upgrade of the experimental environment of BL14.1 and 14.2, which will imply the installation of new X-ray detectors, new cryogenics, new beam diagnostics and a complete new experimental table with samples changer robotics for BL14.1.

With these continous upgrades, we will extend over the course of the coming years our high quality and modern experimental setup, to be used by both the national and international user community.

1. Heinemann, U.; Büssow, C.; Mueller, U. & Umbach, P. , *Acc. Chem. Res.,* **36** (2003) 157-163.

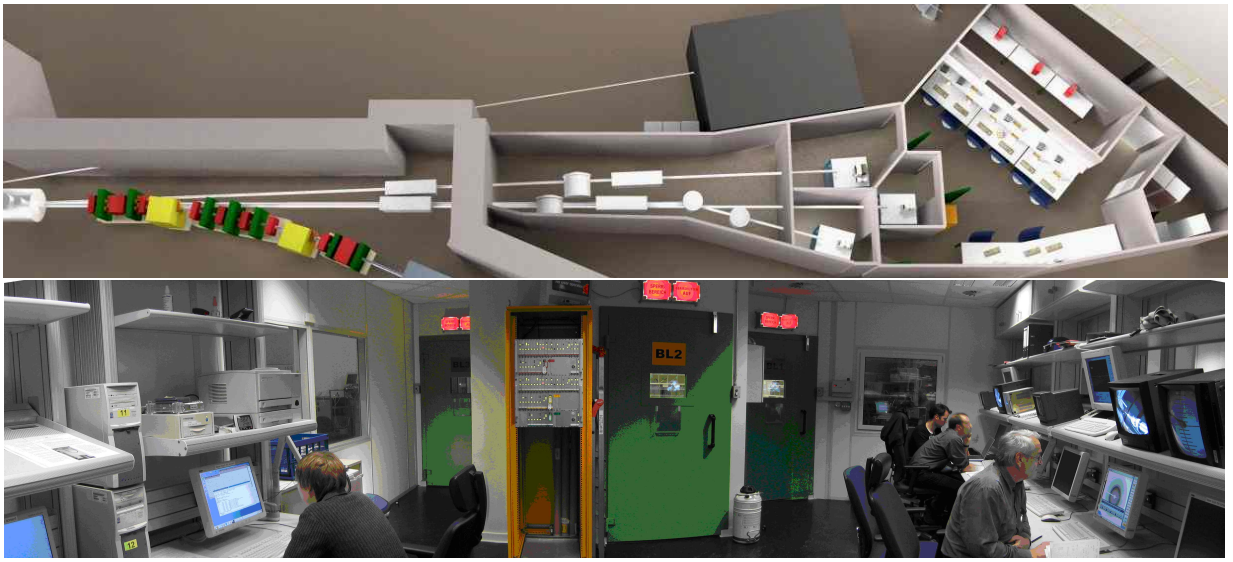

Top: Rendered top-view of the PX-BESSY beamlines. Bottom: Central control room.

L8

AUTOMATED INTERPRETATION OF ELECTRON DENSITY MAPS; ADDING CRYSTALLOGRAPHIC RESTRAINTS TO PROTEIN DESIGN ALGORITHMS

Martin Stiebritz & Yves A. Muller

Lehrstuhl für Biotechnik, Institut für Biologie, Universität Erlangen-Nürnberg

Protein design algorithms based on side chain packing considerations in combination with dead end elimination have proved extremely powerful for the design of proteins with novel properties [1, 2]. Here we present a program which we named MUMBO and which contains most of the features present in the protein design programs reported in the literature [3, 4]. Starting from a given backbone conformation, the program generates all possible side chain rotamers for a list of amino acids at various positions. The combination of rotamers, which represents the global energy minimum of the system, is then selected using the dead end elimination algorithm.

In order to extend the use of the program to the interpretation of electron density maps, we added a subroutine which considers a pseudo energy derived from the electron density present for a certain side chain orientation in a given electron density map. Including this X-ray energy into the dead end elimination algorithm allows for the automated placement of side-chains into the electron density maps while at the same time considering the best possible local side-chain packing environment. At present we explore the use of this approach for the automated model building based on low and high resolution data and using phases from different sources.

1. Looger L L, Dwyer M. A., Smith J. J., Hellinga H. W., *Nature* **423** (2003) 185.
2. Dwyer M. A., Looger L. L., Hellinga H. W., *Science* **304** (2004) 1916.
3. Desmet J., De Maeyer M., Hazes B. and Lasters I., *Nature* **356**, (1992) 539.
4. Goldstein R. F., *Biophys J* **66** (1994) 1335.

Lectures - Friday, September 30

L13

CRYSTAL STRUCTURE OF RNASE PH FROM *BACILLUS STEAROTHERMOPHILUS*

Agnieszka Wojtkowiak[1], Mariusz Jaskólski[1,2]

[1]*Department of Crystallography, Faculty of Chemistry, A.Mickiewicz University, Poznań, Poland*
[2]*Center for Biocrystallographic Research , IBCh, Polish Academy of Sciences, Poznań, Poland*

Maturation of tRNA from longer precursors involves several steps, including the removal of 5' and 3' extension sequences. In bacteria, the 3' processing reactions are carried out by a number of RNases in multistep reactions.

RNase PH is one of the most efficient exoribonucleases that catalyze the final step of the 3' end processing of tRNA in bacteria. This phosphate-dependent enzyme removes nucleotides following the CCA sequence of tRNA precursors, thus generating mature tRNA with amino acid acceptor activity.

RNase PH from the thermophile *Bacillus stearothermophilus* has been crystallized by the hanging drop vapor diffusion method at room temperature from 5.0 mg/ml protein solution containing 0.2 M calcium acetate, 12% v/v PEG3350, and 0.1M HEPES, pH 7.5. Crystals appeared after 2 days and reached maximum dimensions of 0.05 0.10 0.10 mm within 3 days.

Diffraction data were collected at 100 K at Lund, MAX-lab beamline I711, to 3.0 Å resolution. The crystals are trigonal, space group *P*312 with a = 93.0 Å, c = 104.7 Å, and contain two protein molecules in the asymmetric unit, corresponding to a Matthews volume of 2.3 Å^3/Da and 47% solvent content.

The structure has been determinated by molecular replacement using a *Bacillus subtilis* homolog as the search model. The protein forms a hexameric quaternary structure as a trimer of dimers with crystallographic 32 symmetry, and the crystal structure is built up from two such assemblies. The polypeptide chain of the monomer forms a single domain with / fold.¨

L14

CRYSTAL STRUCTURE OF A BACTERIAL CLASS 2 HISTONE DEACETYLASE HOMOLOGUE

T. K. Nielsen[1], C. Hildmann[2], A. Schwienhorst[2], A. Dickmanns[1], R. Ficner[1]

[1]Department of Structural Molecular Biology, Institute for Microbiology and Genetics, Justus-Von-Liebigweg 11, 37077 Goettingen, Germany

[2]Department of Molecular Genetics and Preparative Molecular Biology, Institute for Microbiology and Genetics, Grisebachstr. 8, 37077 Goettingen, Germany

Histone deacetylases (HDACs) are among the most promising new targets for a future cancer therapy. However, structural information that greatly enhances the design of HDAC inhibitors as novel chemotherapeutics is only available on class 1 HDACs so far. Here we present the structure of FB188 HDAH (histone deacetylase-like amidohydrolase from *Bordetella/Alcaligenes* strain FB188) that shows high functional and sequential homology to human class 2 HDACs. FB188 HDAH is capable to remove the acetyl moiety from acetylated -amino groups of lysine residues of histones. Several HDAC inhibitors, which have been shown to inhibit tumor activity in both pre-clinical models and in clinical trials, also actively inhibit FB188 HDAH.

We have detrmined the crystal structure of the first class 2 HDAC homologue, FB188 HDAH, at a resolution of 1.6 Å with bound acetate as well as in complex with the two inhibitors, SAHA and CypX at a resolution of 1.57 Å and 1.75 Å, respectively. FB188 HDAH exhibits the canonical fold of class 1 enzymes with a zinc-ion and two potassium ions bound. The highest diversity compared to known structures of the class 1 enzymes is found in loop regions especially in the area around the entrance of the active site, indicating significant differences of the interacting partners to the class 1 and 2 enzymes. The structures of HDACs and HDAC homologues are prerequisites in the structure based drug design in order to produce more class-specific drugs.

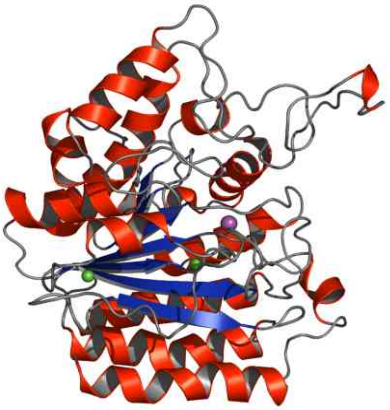

L17

A PATHOGENESIS-RELATED PR-10 PROTEIN WITH MULTIPLE LIGANDS IN BINDING POCKET

Fernandes H., Czyrek W.[1], Pasternak O., Handschuh L., Bujacz G., Sikorski M., Jaskólski M.

Center for Biocrystallographic Research, Poznan, and [1]Technical University of Łódź, - Poland

PR (pathogenesis-related) proteins of class 10 are small (17 KDa), slightly acidic (pI 5), and cytosolic. The main feature of their three-dimentional structure is a seven-stranded antiparallel -sheet, surrounding a long C-terminal helix 3. Between these two structural elements, a large cavity is created [1]. Although the PR-10 proteins are very abundant in the plant kingdom, their physiological role remains unknown. However, recent data indicate that ligand binding could be important for their biological function. It was showed that PR-10 protein from white birch (Betv1) can bind various compounds (including fatty acids, flavonoids and cytokinins) and NMR data indicated that binding occurs in the internal cavity. Crystallographic studies have also showed that Betv1 proteins bind two deoxycholate molecules in the cavity.

The present study of the yellow lupine LlPR-10.2B protein in complex with a plant hormone – zeatin is another example for the capability of PR-10 protein to bind ligands. This kind of ligand binding has been already reported for a plant cytokinin-specific binding protein (CSBP) [2], and recently the structure of another PR-10 protein (LlPR-10.2F) has been solved in complex with a synthetic cytokinin. The present crystal structure has been solved by molecular-replacement using X-ray diffraction data extended to 1.4 Å resolution (Figure 1). The structure reveals that a single LlPR-10.2B molecule is capable of binding four zeatin ligands.

Three of the zeatin molecules are located in the binding cavity and one zeatin molecule is shared by two symmetry-related protein chains. The ligand molecules could be

unambiguously modeled since the corresponding electron density was of excellent quality.

1. J. Biesiadka, G. Bujacz, M. M. Sikorski, M. Jaskolski, *J. Mol. Biol.* **319**(5), 1223-34 (2002).

2. G. D. Bujacz, O. Pasternak, Y. Fujimoto, Y. Hashimoto, M. M. Sikorski, M. Jaskolski, *Acta Cryst.* **D59**, 522-525 (2003).

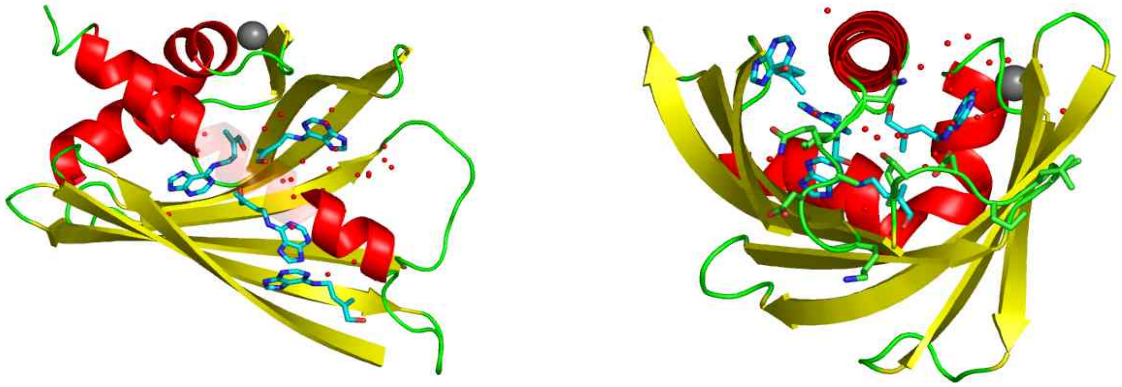

Figure 1. The overall fold of LlPR-10.2B protein showed in two distinct perspectives.

L18

STRUCTURAL INSIGHT INTO THE INDUCTION OF THE BACTERIAL REPRESSOR TETR BY THE AGONISTE PEPTIDE TIP

Sylvia R. Luckner[1], Michael Klieber[1], Marcus Klotzsche[2], Wolfgang Hillen[2] & Yves A. Muller[1]

[1]Lehrstuhl für Biotechnik and [2]Lehrstuhl für Mikrobiologie, Institut für Biologie, Friedrich-Alexander-Universität Erlangen-Nürnberg

Tailored peptides show large promise for clinical and biotechnological applications, and are able to generate unprecedented insight into the mechanisms of protein regulation and activation. A caveat of standard *in vitro* selection procedures is that most peptide sequences obtained by phage display or mRNA display function as inhibitors of protein action [1].

The recently discovered peptide Tip [2] not only represents a rare example of an agoniste peptide but in addition its function appears significantly more sophisticated than that of other agonist peptides. Whereas the latter limit themselves to directly or indirectly promoting protein interactions [3], Tip is able to trigger an allosteric switch in the bacterial repressor TetR and thereby to substitute for the natural effector tetracyline (Tc). Tip switches the conformation of TetR between a DNA-binding competent form that represses gene transcription and a non-DNA-binding conformation that dissociates TetR [4] from its operator DNA so that gene transcription can take place. Because of the fundamental importance of the regulation of gene expression and because TetR is a widely used tool to study gene transcription in prokaryotes and eukaryotes [5], we used crystallography to unravel the atomic mechanism by which Tip trips the allosteric switch.

1. Dower WJ and Mattheakis LC, *Curr Opin Chem Biol* **6** (2002) 390.

2. Klotzsche M, Berens C and Hillen W, *J Biol Chem* (2005).

3. Wrighton NC et al., *Science* **273** (1996) 458-64.

4. Saenger W, Orth P, Kisker C, Hillen W and Hinrichs W, *Angew Chem Int Ed Engl* **39** (2000) 2042.

5. Berens C and Hillen W, *Eur J Biochem* **270** (2003) 3109.

L20

STRUCTURE-BASED RE-ENGINEERING OF INTERNALIN – THE INTESTINAL INVASIN OF *LISTERIA MONOCYTOGENES*

Thomas Wollert, Dirk W. Heinz, Wolf-Dieter Schubert

German Research Centre for Biotechnology, Braunschweig, Germany

The food-borne pathogen *Listeria monocytogenes* causes severe infections in immunocompromised patients. At 30%, the mortality rate of this pathogen far exceeds that of other common food-borne pathogens such as *Samonella enteritidis* or *Vibrio species*. The first step of listerial infection involves the uptake of bacteria into normally nonphagocytotic epithelial cells of the intestine. This uptake is mediated by the interaction of the major invasin of this bacterium, Internalin (InlA), with its human receptor E-Cadherin.

We have previously investigated the recognition complex of InlA and human E-cadherin structurally by crystallizing the complex between functional fragments of both proteins. The leucine-rich-repeat (LRR) protein InlA was found to bind the N-terminal domain of E-cadherin through its 15 unit LRR-domain. Nevertheless, despite a large interaction surface, the complex is surprisingly weak - especially when compared to complexes with interaction surfaces of comparable size.

The weak interaction makes this complex an ideal tool to study and quantify the contribution of individual amino acid residues to the overall binding affinity. We have therefore re-engineered the complex, by replacing individual residues by point mutation - in InlA only. As a result, we

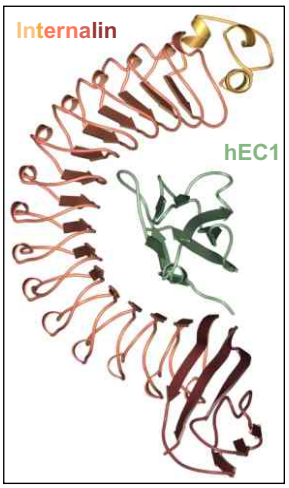

have been able to increase the affinity by up to 6600 fold - by merely replacing two amino acid residues. Using isothermal titration calorimetry, we have furthermore been able to quantify the thermodynamics of the interaction and evaluate the effects of single hydrogen bonds and other interactions in detail.

L21

THE 1.9 Å X-RAY STRUCTURE OF THE RV2827C PROTEIN FROM *MYCOBACTERIUM TUBERCULOSIS*

Robert Janowski, Santosh Panjikar, Jochen Müller-Dieckmann and Manfred S. Weiss

European Molecular Biology Laboratory, Notkestrasse 85, D-22603 Hamburg, Germany

Tuberculosis (TB) is the single leading cause of human adult death by an infectious organism. It accounts for over 2 million deaths per year, primarily in the developing world. Multi-drug resistant Mycobacterium tuberculosis strains are increasingly being found in the clinic. Early treatment with at least two effective drugs (isoniazid, rifampicin) can often reduce mortality with multi-drug resistant tuberculosis, but outbreaks of tuberculosis with strains resistant to seven or more drugs have been reported. It appears likely that strains which are completely resistant to existing antibiotics will become increasingly common. It points to the critical need for new drugs that are active against alternative targets.

The objective of our research project is to obtain structural information on proteins from M. tuberculosis identified by expression profiling and mRNA analysis, by which the different stages of life of this pathogenic bacterium can be distinguished. These proteins may also play an important role in its pathogenesis. The structural information on such proteins from M. tuberculosis is limited to date. Therefore, the elucidation of 3D structures would provide important information on the biochemical functions of the molecules. This will constitute a valuable basis for understanding pathogenesis and for structure-based design of the new drugs.

Rv2827c from M. tuberculosis does not show any significant amino acid sequence similarity to other known proteins (except to its homologues in M. bovis and M. mikroti). The structure of this hypothetical protein has been solved using the MAD technique (quick bromide soaking, 25 bromide sites in the asymmetric unit) to a resolution of 2.6 Å and afterwards it has been refined using native data collected to 1.93 Å resolution. The structure is composed of 2 or 3 domains. The C-terminal fragment (83-295 aa) is

not reminiscent of any other 3D structure based on a comparison done using the DALI and SSM servers.

The N-terminal part of Rv2827c (1-82 aa) is definitely a separate domain and consists of a winged-helix (or helix-turn-helix) motif. According to the results from the DALI and SSM servers its fold (15-74 aa fragment) is common for several different types of the proteins responsible for DNA/RNA binding (transcription regulators). Very interesting is the fact that the structure of this fragment is similar to two proteins responsible for an antibiotic resistance regulation (methicillin resistance regulating transcriptional repressor from S. aureus, and multiple antibiotic resistance repressor from E. coli). Based on the structural comparison of the N-terminal domain we assume that the Rv2827c protein plays a role in the regulation of the transcription. DNA binding experiments are in progress.

L23

CRYSTAL STRUCTURES OF TWO ALCALASE COMPLEXES: WITH NATIVE CI-2A INHIBITOR AND M59P MUTANT AT ULTRA HIGH RESOLUTION (0.74 Å)

Joanna Raczyńska[1], Robert Jędrzejczak[2], Peter Oestergard[3], Wojciech Rypniewski[1]

[1]Institute of Bioorganic Chemistry, Polish Academy of Sciences, Poznan, Poland
[2]Argonne National Laboratory, USA
[3]Novozymes, Denmark

Alcalase® is a serine protease of the subtilisin family. It is a naturally occuring variant[1] of subtilisin Carlsberg[2], prepared commercially from a selected strain of Bacillus licheniformis. The inhibitor presented here is the chymotrypsin inhibitor 2A (CI-2A) from the seeds of the Hiproly strain of barley. It is a member of the potato inhibitor I family of serine proteases inhibitors[3]. It is worth noting, that it is a competitive inhibitor of chymotrypsin and subtilisin but not of trypsin by which it is cleaved[4].

The inhibitor is bound to the enzyme via short antiparallel beta-sheet interactions, Van der Waals contacts of the P1 residue with the binding pocket of the protease and also interactions (mainly H-bonds) on the side of a potential leaving part of the inhibitor.

The main differences between the two complexes are at the binding site. Mutation from methionine to proline at the P1 position causes the weakening of the Van der Waals interactions within the binding pocket of the protease.

Both structures cointain a high proportion of residues having double conformations, including a few segments of the main chain. Large number of disordered residues is often seen in structures solved from low temperature data and such details can be easily analysed when high resolution data are available.

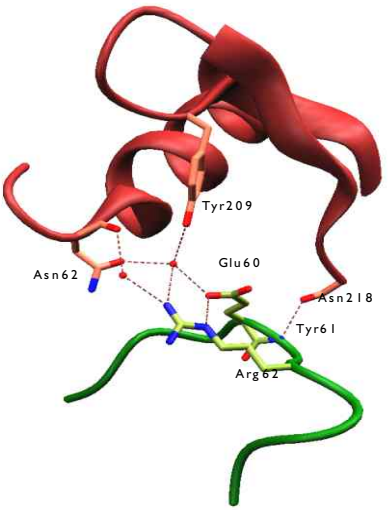

Figure 1. H-bonding interactions between the enzyme (red) and the inhibitor (green).

1. Jacobs, M., Eliasson, M., Uhlen, M. and Flick, J. I. (1985) *Nucleic Acids Res*. **13**, 8913-26.
2. Liderstrom-Lang, K. And Ottesen, M. (1947) *Nature* **159**, 807-808.
3. Jonassen, I. (1980) *Carlsberg Res. Commun*. **45**, 47-58.
4. Longstaff, C., Campbell, A. F. and Fersht, A. R. (1990) *Biochemistry* **29**, 7339-47.

L24

CRYSTAL STRUCTURE OF PA0740, A NOVEL ZINC-DEPENDENT SULFATASE FROM THE HUMAN PATHOGEN *PSEUDOMONAS AERUGINOSA*

Gregor Hagelüken[1], Thorsten Adams[2], Lutz Wiehlmann[3], Harald Kolmar[2], Burkhardt Tümmler[3], Dirk W. Heinz[1], Wolf-Dieter Schubert[1]

[1]German Research Center for Biotechnology, Braunschweig, Germany
[2]University of Göttingen, Department of Microbiology and Genetics
[3]Hannover Medical School, Germany, [*]E-mail: wds@gbf.de

Sulfur is the fifth most common element in organic compounds after carbon, oxygen, nitrogen and hydrogen. Though sulfur is generally available in the biosphere in the form of organic compounds, free sulfate ions are frequently growth limiting. In particular sulfur ester compounds, ubiquitously produced by living organisms and hence found in throughout the biosphere, account for a large fraction of sulfur content in aerobic soils.

Microorganisms can utilize these sulfur esters as their sole source of sulfur for growth using sulfatases, of widely varying substrate specificities. Three mechanistically distinct groups of sulfatases have been identified - each unrelated to the other two:

Arylsulfatases, the best-studied group (group I), are predominantly eukaryotic but occur in some prokaryotes, as well. They are characterized by a serine or cysteine post–translationally modified to a formylglycine that nucleophilically attacks the sulfate ester, producing inorganic sulfate and the corresponding alcohol.

The second group belongs to the Fe(II) a-ketoglutarate-dependent di-oxygenase superfamily of enzymes. These enzymes oxidatively cleave sulfate esters into inorganic sulfate and the corresponding aldehyde and require a-ketoglutarate as a co-substrate. The only crystal structure of this group is that of AtsK of *Pseudomonas putida*.

PA0740 belongs to a third, as yet poorly characterized group of sulfatases. Their N-terminal domain contains a Zn^{2+} binding motif (S/T**H**x**H**x**DH**xG**G**) similar to one in

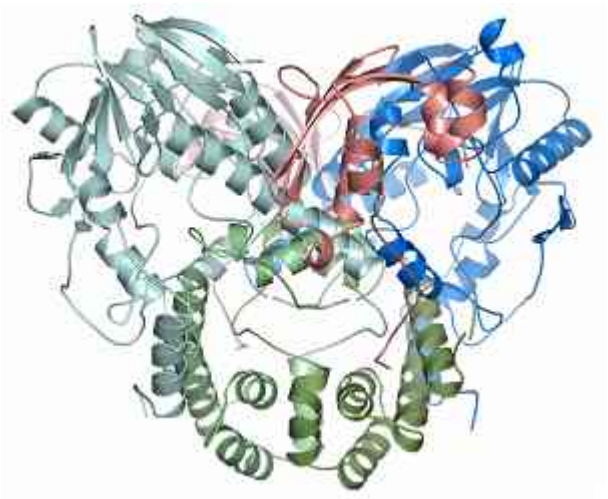

class B -lactamases. We have solved the crystal structure of PA0740, a member of this group, at 1.8 Å resolution.

PA0740 is a symmetric dimer, with an unusual a-helical dimer interface that intricately interlocks the monomers. Each monomer furthermore contains an N-terminal abba-sandwich domain reminiscent of class B b-lactamases. The central domain of PA0740 is involved in dimerization, while the C-terminal domain is structurally similar to sterol carrier protein-2.

L25

CRYSTALLOGRAPHIC STUDIES ON THE 2-OXOGLUTARATE DEPENDENT OXYGENASE RDPA

J. Kraußе[1], A. Westendorf[2], E.B. Küttner[1], R.H. Müller[2], N. Sträter[1]

[1]Centre for Biotechnology and Biomedicine, University Leipzig, Deutscher Platz 5, D-04103 Leipzig, Germany
[2]UFZ Centre for Environmental Research, 15, D-04318 Leipzig, Germany

The most widespread group of mononuclear non-heme iron enzymes is the family of 2-oxoglutarate (2-OG) dependent oxygenases. Its members are found in bacteria as well as eukaryotes and catalyze a large variety of reactions. The catalysis is always coupled with the decarboxylation of 2-OG and the consumption of molecular oxygen. A 2-OG dependent oxygenase was isolated from *Delftia acidovorans* MC1. It carries enantiospecific activity for the etherolytic cleavage of R-(2,4-dichlorophenoxy)propionate (Rdp) and is thus referred to as RdpA. Its substrate belongs to the group of chlorinated phenoxyalkanoates which were widely used herbicides in agriculture and remain as severe soil pollutants. The crystal structure of RdpA is of special interest to analyze its stereospecific substrate recognition in comparison to a homologous enzyme (SdpA) which catalyzes the decomposition of S-(2,4- dichlorophenoxy)propionate (Sdp) exclusively. Such knowledge would possibly allow for the design of new specific catalysts.

Initial crystallization conditions for RdpA were found by sparse matrix method. Refinement was carried out to obtain crystals suitable for X-ray diffraction experiments. Data collection was performed at BESSY, Berlin. The crystals of native RdpA show strongly anisotropic diffraction up to 2.5 Å resolution. They are well ordered along the b and c axes. Along the poorly ordered a-axis they diffract to 3.2 Å. The structure was determined at 2.9 Å by molecular replacement in space group $C222_1$ using the homologous protein TauD from *E. coli* as phasing model. The assymetric unit probably contains two dimers of the enzyme. To enhance protein propensity for crystallization and consequently crystal quality, surface mutagenesis was carried out. Lysyl and glutamyl residues were substituted by alanine to lower conformational entropy and mediate crystal contacts.

1. Westendorf, A. *et al.* (2002) *Microbiol. Res.* **157**, 317-322.
2. Westendorf, A. *et al.* (2003) *Acta Biotechnol.* **23**, 3-17.

Lectures - Saturday, October 1

L26

A SERINE PEPTIDASE WITH A SER-HIS-GLU TRIAD AND A NUCLEOPHILIC ELBOW

Henryk J. Korza[1,2] and Matthias Bochtler[1,2]

[1]International Institute of Molecular and Cell Biology,ul. Trojdena 4, 02-109 Warsaw, Poland
[2]Max-Planck-Institute for Molecular Cell Biology and Genetics,Pfotenhauerstr. 108, 01309 Dresden, Germany

LD-carboxypeptidases (EC 3.4.17.13) are named for their ability to cleave amide bonds between L- and D-amino acids, which occur naturally in bacterial peptidoglycan. They are specific for the link between meso-diaminopimelic acid and D-alanine, and therefore degrade NAG-NAM tetrapeptides to the corresponding tripeptides. As only the tripeptides can be reused as peptidoglycan building blocks, LD-carboxypeptidases are thought to play a role in peptidoglycan recycling. Despite the pharmaceutical interest in peptidoglycan biosynthesis, the fold and catalytic type of LD-carboxypeptidases are unknown. Here, we show that a previously uncharacterized open reading frame in *Pseudomonas aeruginosa* has LD-carboxypeptidase activity and present the crystal structure of this enzyme. The structure shows that the enzyme consists of an N-terminal -sheet and a C-terminal -barrel domain. At the interface of the two domains, serine 115 adopts a highly strained conformation in the context of a strand-turn-helix motif that is similar to the "nucleophilic elbow" in -hydrolases. This serine residue is hydrogen-bonded to a histidine residue, which is oriented by a glutamate residue. All three residues, which occur in the order serine, glutamate, histidine in the amino acid sequence, are strictly conserved in naturally occurring LD-carboxypeptidases and cannot be mutated to alanines without loss of activity. We conclude that LD-carboxypeptidases are serine peptidases with serine, histidine, glutamate catalytic triads.

L27

MOLECULAR BASIS FOR MULTIPLE SULFATASE DEFICIENCY AND CATALYTIC MECHANISM FOR FORMYLGLYCINE GENERATION OF THE HUMAN FORMYLGLYCINE GENERATING ENZYME

Dirk Röser[1], Achim Dickmanns[1], Kurt von Figura[2], Ralf Ficner[1], and Markus G. Rudolph[1]

[1]Abt. Molekulare Strukturbiologie, Institut für Mikrobiologie und Genetik, Georg-August-Universität, Justus-von-Liebig Weg 11, D-37077 Göttingen
[2]Abt. Biochemie II, Georg-August-Universität, Heinrich-Düker-Weg 12, D-37073 Göttingen

Sulfatases use formylglycine (FGly) as the key catalytic residue in their active site to hydrolyze sulfate esters. FGly is unique to sulfatases and is post-translationally generated from cysteine by FGE, the formylglycine generating enzyme. The precise mechanism for FGly generation is unknown but involves disulfide bond formation and requires calcium, molecular oxygen, and a reducing agent. Inactivity of FGE due to inherited mutations results in multiple sulfatase deficiency (MSD), a severe syndrome that leads to early death in infants.

The crystal structure of the FGE paralogue, pFGE, was determined previously (Dickmanns *et al.*) and was used to determine several crystal structures of FGE by molecular replacement. The FGE structure could also be determined *de novo* by a combination of Calcium/Sulfur SAD phasing and density modification (Roeser *et al.*). These structures provide insight into the catalytic mechanism of FGly generation and establish the molecular basis for MSD. The structure of FGE explains the effect of the various point mutations found in MSD patients. Some mutations

destabilize FGE, while others render metal binding impossible or substitute catalytically important residues.

Six structures of wild-type FGE in the apo form revealed a redox-active disulfide bond at the bottom of a cleft that was proven to be the substrate binding site by a cocrystal structure of an FGE mutant and substrate peptide. Most strikingly, an oxidized cysteine residue, possibly cysteine sulfenic acid, is present in several structures of FGE, which could represent a catalytically relevant intermediate. The FGE structures provide the basis for a complete description of the FGE catalytic cycle on the way to reactivation of sulfatase activities in MSD patients (Dierks *et al.*).

In contrast to FGE, pFGE lacks FGly-generating activity but nevertheless binds peptides that are substrates for FGE. Interestingly, pFGE crystallizes as a dimer with the substrate binding sites buried. As the function of pFGE is likely related to FGE activity (Mariappan *et al.*), FGE/pFGE heterodimer formation is conceivable, even with a substrate bound to FGE. Such a complex could serve a regulatory function that has still to be elucidated.

1. Dickmanns *et al.* (2005). Crystal Structure of Human pFGE, the Paralog of the C -formylglycine-generating Enzyme. *J Biol Chem* **280**(15): 15180-15187.
2. Dierks *et al.* (2005). Molecular basis for multiple sulfatase deficiency and mechanism for formylglycine generation of the human formylglycine-generating enzyme. *Cell* **121**(4): 541-552.
3. Mariappan *et al.* (2005). Expression, Localization, Structural, and Functional Characterization of pFGE, the Paralog of the C -Formylglycine-generating Enzyme. *J Biol Chem* **280**(15): 15173-15179.
4. Roeser *et al.* (2005). "De novo calcium/sulfur SAD phasing of the human formylglycine generating enzyme using in-house data." *Acta Cryst.* **D61**: in press.

L28

DHC2 – A NOVEL DIHEME CYTOCHROME *C* FROM *GEOBACTER SULFURREDUCENS*

Heitmann, D.[1], Einsle, O.[1]

[1]Molecular Structural Biology, Institute for Microbiology and Genetics; University of Göttingen

Multiheme cytochromes of the *c* type are a widespread class of proteins with a variety of functions in electron transport and enzymatic catalysis In multi-heme cytochromes not only the attachment of the prosthetic groups to the protein backbone is of importance, but also the arrangement of hemes in respect to each other. Conservation of two different heme arrangement motifs has been observed, showing a parallel and a perpendicular interaction and implicating that a functional reason for fixing special heme geometries over several enzymes and species exists. These cytochrome catalyzed reactions are of major importance for bacterial life, as for example the conversions performed by the large redox enzymes hydroxylamine oxidoreductase (HAO) or cytochrome *c* nitrite reductase (ccNiR).

Although many multiheme *c*-type cytochromes have been analyzed by a variety of techniques, none of these studies could conclusively demonstrate how the structurally conserved arrangements of functional heme groups are able to establish enzymatic functionality in the way they do. Because their redox chains consist of more than two heme groups, the data shows overlapping signals resulting from interaction of more than two heme groups, averting examination of interactions of only one motif. Focusing of spectroscopic and redox potential data on one of these heme arrangements is a problem that cannot be overcome by most systems.

Here we describe the biochemical and X-ray crystallographic characterization of the 94 amino acid containing diheme cytochrome DHC2, showing a novel protein fold in combination with a parallel heme packing motif and unusual heme group parameters. By joining redox potentiometry, EPR, visible spectroscopy, site directed mutagenesis and x-ray crystallographic structures the features of parallel heme motifs can be approached in a broad systematical way, revealing the mechanisms in which this functional motif acts in multiheme proteins.

1. Pettigrew, G. W. & Moore, G. R. (1987). *Cytochromes c. Biological aspects*, Springer Verlag KG, Berlin, Germany.
2. Stevens, J., Daltrop, O., Allen, J. & Ferguson, S. (2004). C-type cytochrome formation: Chemical and biological enigmas. *Acc. Chem. Res.* **37**, 999-1007.
3. Igarashi, N., Moriyama, H., Fujiwara, T., Fukumori, Y. & Tanaka, N. (1997). The 2.8 Ĺ structure of hydroxylamine oxidoreductase from a nitrifying chemoautotrophic bacterium, *Nitrosomonas europaea*. *Nat. Struct. Biol.* **4**, 276-284.
4. Einsle, O. (2001). Cytochrome *c* nitrite reductase. In *Handbook of Metalloproteins* (Messerschmidt, A., Huber, R., Poulos, T. & Wieghardt, K., eds.). Wiley & Sons, NewYork.

L29

CRYSTAL STRUCTURE OF THE TYPE III SECRETION CHAPERONE SYCT FROM *YERSINIA ENTEROCOLITICA*

Carina R. Büttner, Dirk W. Heinz, Hartmut H. Niemann

Division of Structural Biology, German Research Centre for Biotechnology, Mascheroder Weg 1, D-38100 Braunschweig, Germany

Pathogenic *Yersinia* ssp. use the type III secretion (TTS) system to inject cytotoxic effector proteins directly into the mammalian host cell. To be effectively translocated, several of these effectors require transient binding to specific chaperones in the bacterial cytoplasm. SycT is the chaperone of YopT, a 36 kDa cysteine protease that cleaves the C-terminal membrane-anchor of Rho-GTPases of the host organism. The lack of GTPase signaling for actin polymerization leads to disruption of actin stress fibers and impedes the formation of phagocytotic cups contributing to the anti-phagocytotic effect of *Yersinia*. We determined the crystal structure of 15 kDa SycT from three crystal forms. SycT forms a homodimer with an overall fold similar to other TTS effector chaperones. Two hydrophobic patches involved in effector binding in other TTS effector chaperones are also found in SycT . In the absence of the effector, these patches interact with the hydrophobic C-terminal peptide of the chaperone and are involved in crystal contacts. SycT exhibits distinct differences compared to other TTS chaperones (e.g. SycE): SycT lacks the dimerization helix and has an additional -strand resulting in a more compact shape. This additional -strand is capable of undergoing a conformational change that might be required for effector binding.

Biochemical analyses of the complex between SycT and YopT reveal a stoichiometric chaperone:effector ratio of 2:1. The chaperone-binding site comprises at least residues 52 to 103 of YopT.

L30

CRYSTAL STRUCTURE OF FUCOSYLTRANSFERASE FROM *BRADYRHIZOBIUM*

Krzysztof Brzezinski[1], Tomasz Stepkowski[2], Grzegorz Bujacz[2,3], Santosh Panjikar[4], Mariusz Jaskolski[1,2]

[1]Department of Crystallography, Faculty of Chemistry, A. Mickiewicz University, Grunwaldzka 6, 60-780 Poznan, Poland

[2]Institute of Bioorganic Chemistry, Polish Academy of Sciences, Noskowskiego 12/14, 61-704 Poznan, Poland

[3]Institute of Technical Biochemistry, Technical University of Lodz, Stefanowskiego 4/10, 93-923 Lodz, Poland

[4]EMBL Hamburg, Notkestrasse 85, 22603 Hamburg, Germany

Symbiosis between legume plants and *Rhizobium* bacteria depends on exchange of specific molecular signals. This process results in the formation of root nodules in which the bacteria fix atmospheric nitrogen. In the initial phases of nodulation, the host plant secrets flavonoids and activation of bacterial *nod* genes is induced. The *nod* genes are involved in the synthesis of lipochitin oligosaccharides, called Nod factors, which are necessary for infection of root hair by the symbiotic bacteria. One of the steps during the synthesis of the Nod factors is an attachment of L-fucose, catalyzed by an enzyme, NodZ fucosyltransferse.

The coding seqence of the *nodZ* gene was amplified by PCR from genomic DNA of *Bradyrhizobium*. A C-terminal $(His)_6$-tag sequence was introduced by a nucleotide primer. The tagged gene was cloned into the pET3a vector and expressed in *Escherichia coli* BL21 CodonPlus RIPL cells. Soluble protein was purified by nickel-NTA affinity chromatography and gel filtration. The His-tag was not removed for crystallization. Selenomethionyl NodZ was obtained by inhibition of the methionine biosynthetic pathway with the same expression vector and *Escherichia coli* strain as for the native protein. Purification of Se-Met NodZ was carried out using the same protocol as for the wild-type NodZ. Mass spectrometry analysis of Se-Met substitution of the six methionine sites showed high substitution levels. Crystals of NodZ with several habits were obtained at 19 and 4°C by the hanging drop vapor diffusion method with KH_2PO_4 as precipitant. Se-Met NodZ was crystallized at 19°C using a similar protocol. The native crystals are hexagonal, space group $P6_522$, with a = 125.5, c = 95.6 Å (form I) or a = 130.1, c = 83.3 Å (form II), and contain one protein molecule in the asymmetric unit. The crystals of Se-Met NodZ are isomorphous with form I. Multiwavelength anomalous diffraction (MAD) data for Se-Met NodZ were collected at three wavelengths around the selenium *K* absorption edge using synchrotron radiation. The MAD data were used to solve the structure of forms I of NodZ. The diffraction data extend to 1.54 (form I), 1.95 (form II), and 2.4 Å (Se-Met derivative).

Stereochemically restrained structure-factor refinement (maximum likelihood targets) of both structures has converged with very good model parameters and R/R_{free} factors of 18.8 / 19.9% (form I) and 15.8 / 18.9% (form II).

The fold of NodZ consists of 12 strands (S1-S12) and 12 helices (H1-H12), which can be arranged into two domains of nearly equal size. Domain 1 contains 7 helices (including 3_{10} helices H3, H4, and H5) and 6 strands. Domain 2 contains 6 strands and 5 helices. The two domains share a similar fold, however their topology (connectivity) is different. In domain 2, the secondary structure elements are arranged into a variant of Rossmann fold. Although the sequence contains ten cysteine residues, they are not paired into disulfide bridges. Three proline residues (83, 86 and 284) are in *cis* conformation. Although there is no sequence similarity to other glycosyltransferases, NodZ is structurally similar to BGT, which defines the fold of one of the two families of glycosyltransferases.

L31

THE STRUCTURE OF YEAST PHOSPHOFRUCTOKINASE 1

Katarzyna Banaszak[1], Ingrid Attinost[2], Gerhard Kopperschlaeger[3], Wojciech Rypniewski[1]

[1]Institute of Bioorganic Chemistry, Polish Academy of Science, Poland
[2]EMBL, Hamburg, Germany
[3]Institute of Biochemistry, Leipzig University, Germany

6-Phosphofructo-1-kinase (Pfk), a key enzyme in glycolysis, is a heterooctamer ($_4$ $_4$) of about 800 kDa (21S). The crystal structure of the limited proteolysis product (600 kDa, 12S Pfk) was determined to 2.9 Å resolution. The total number of atoms of the Pfk model exceeds 44,000 and subsequently the number of parameters to be refined is four times as many. Owing to the low data to parameter ratio at this resolution (172,763 unique reflections have been obtained) the refinement has been carried out under tight restraints and with careful monitoring of the R/R_{free} ratio. The bulk of the molecule has clear electron density.

Fructose-6-phosphate was present in the crystallization medium. The electron density clearly shows the mode of binding of the ligand in the active site and in the binding site of the allosteric effector: fructose-2,6-bisphosphate, unique to eukariotic Pfk. The Pfk molecule appears to be in the allosteric R-state.

L32

THE CRYSTAL STRUCTURE OF THE PYRUVATE DECARBOXYLASE FROM *KLUYVEROMYCES LACTIS* – NEW IMPLICATIONS FOR THE SUBSTRATE ACTIVATION MECHANISM

Steffen Kutter[1], Sandy Relle[1], Michael Spinka[1], Georg Wille[1], Manfred S. Weiss[2], Gerhard Hübner[1] and Stephan König[1]

[1]Institute of Biochemistry, Dept. Biochemistry & Biotechnology, Martin-Luther-University Halle-Wittenberg, Halle (Saale), Germany
[2]European Molecular Biology Laboratory (EMBL c/o DESY), Hamburg Outstation, Germany

The crystal structure of the thiamine diphosphate dependent enzyme pyruvate decarboxylase from *Kluyveromyces lactis* (*Kl*PDC) has been determined to 2.26 Å. The model could be refined to an R-factor of 0.163 and an R_{free} value of 0.230. The asymmetric unit (space group $P12_11$) contains four identical subunits arranged as a dimer of dimers. This quaternary structure represents the catalytically active form of the enzyme. The cofactor thiamine diphosphate is bound in its so-called "V"-conformation to the active site of each subunit. Each monomer can be divided into three domains, each with a/b topology and high structural homology to pyruvate decarboxylase from *Saccharomyces cerevisiae* (*Sc*PDC) [1] and other thiamine diphosphate dependent enzymes. In contrast to the solvent accessible substrate binding sites in *Sc*PDC, two of the four active sites of *Kl*PDC are found in a closed conformation caused by the mutual rotation of the dimers in the tetramer. A similar arrangement has been described for *Sc*PDC crystallized in the presence of the substrate surrogate pyruvamide (PA*Sc*PDC) [2]. There are two disordered loop regions in *Kl*PDC comprising residues 104-115 and 288-302 in each subunit. Despite the different dimer arrangement of both enzymes within the tetramer , the same regions were omitted from the crystal structure model of *Sc*PDC. Pyruvamide binding at *Sc*PDC caused ordering of one half of the loops limiting the access to two active sites. Analysis of the crystal structure models of ScPDC, PAScPDC and KlPDC, comparison of the amino acid composition of the interface area of dimers as well as small angle X-ray solution scattering data of these PDC species imply that the substrate activation involves ordering of the loop regions 104-115 and 288-302.

1. Arjunan, P., Umland, T., Dyda, F., Swaminathan, S., Furey, W., Sax, M., Farrenkopf, B., Gao, Y., Zhang, D. &

Jordan, F. (1996) Crystal structure of the thiamin diphosphate-dependent enzyme pyruvate decarboxylase from the yeast *Saccharomyces cerevisiae* at 2.3 Ĺ resolution. *J. Mol. Biol.* **256**, 590-600.

2. Lu, G., Dobritzsch, D., Baumann, S., Schneider, G. & König, S. (2000) The structural basis of substrate activation in yeast pyruvate decarboxylase - A crystallographic and kinetic study. *Eur. J. Biochem.* **267**, 861-868.

L33

ENZYMES IN ACTION X-RAY CRYSTALLOGRAPHIC SNAPSHOTS OF THE THIAMINE DIPHOSPHATE DEPENDENT PYRUVATE OXIDASE FROM *LACTOBACILLUS PLANTARUM*

D. Meyer, G. Wille, S. König, G. Hübner & K. Tittmann

Institute of Biochemistry, Dept. Biochemistry & Biotechnology, Martin-Luther-University Halle-Wittenberg Kurt-Mothes-Str.3, 06020 Halle/Saale, Germany

The thiamine diphosphate and flavin dependent pyruvate oxidases are enzymes of the energy metabolism of some prokaryotic organisms, e.g. *E. coli* and *L. plantarum*. The *Lactobacillus* enzyme (*Lp*POX) converts pyruvate under consumption of oxygen and phosphate into the high-energy metabolite acetyl phosphate. Due to the high potential for a phosphate-transfer this compound can be subsequently used for the generation of ATP by an acetate kinase.

With the help of stopped-flow kinetics and a method for the determination of the distribution of the intermediates based on proton NMR spectroscopy, we could identify a wild type-like variant which enabled us to solve the structures of complexes of *Lp*POX with two native-like intermediates (lactyl-thiamine diphosphate and hydroxyethyl-thiamine diphosphate) and one non-physiological intermediate (acetyl-thiamine diphosphate) by soaking crystals in exactly defined substrate solutions.

The obtained snapshots provide insights into the reaction mechanism of this enzyme on an atomic scale and throw some light on some features of thiamine diphosphate mediated catalysis discussed for a long time. One of these features is the perpendicular orientation of the carboxylate group in lactyl- thiamine diphosphate, which is postulated to be necessary for the subsequent decarboxylation of this intermediate.

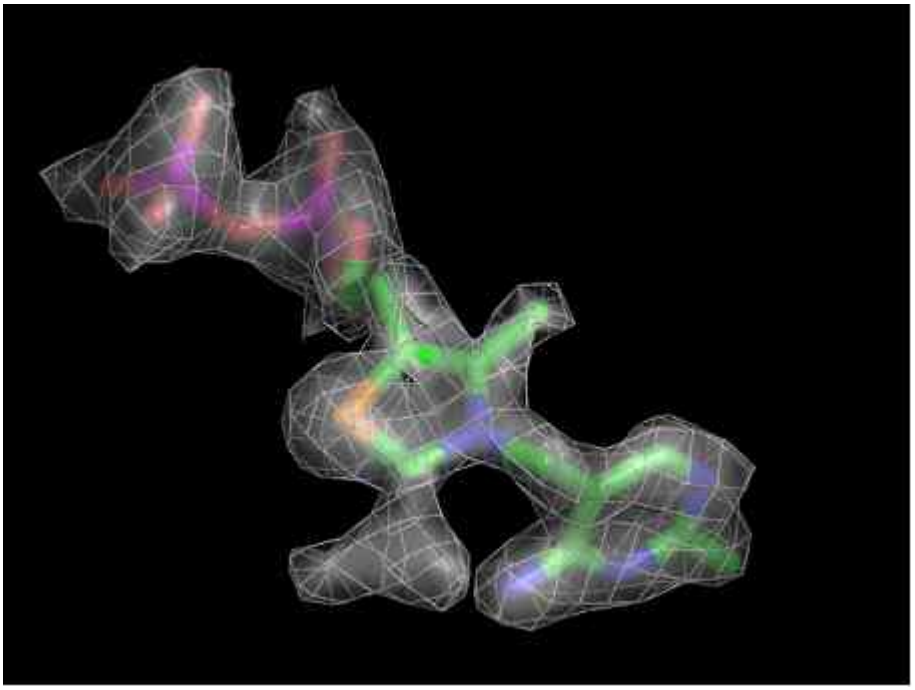

Additional electron density attached to the C2-atom of thiamine diphosphate in the active site of an *Lp*POX-variant reveals a trapped intermediate.